JOURNAL OF MATERIALS SCIENCE 28 (1993) 4510–4514

Local variations of the dynamic elastic modulus around running cracks

P. S. THEOCARIS
National Academy of Athens, P. O. Box 77230, Athens 175-10, Greece
N. P. ANDRIANOPOULOS, S. K. KOURKOULIS
Department of Engineering Sciences, Athens National Technical University, 5 Heroes of Polytechnion Avenue, 157-73 Greece

The variation of the dynamic elastic modulus in the immediate vicinity of the tip of the running crack was studied through an iterative procedure, based on the theoretical expressions for the stress-field components and the experimental relation between strain rate and elastic modulus. It was found that the elastic modulus varied strongly around the tip of the crack, both in radial and polar sense. Also it was observed that the polar distribution of the elastic modulus presented clear off-axis extrema in directions that were in good agreement with experimentally measured branching angles, thus indicating a possible relation between these two phenomena.

1. Introduction

It is known that most mechanical properties of materials show a strong dependence on strain rate. Attempts to relate strain rates with mechanical properties and especially with variations of elastic modulus were presented a few decades ago. For example, one of the most important experimental works is that by Marshall [1], who obtained the stress optical coefficient and the elastic modulus under dynamic loading conditions, whilst of the theoretical works that of Theocaris and Georgiades [2] should be mentioned. In general, however, the systematic exploitation of these results has been restricted, until now, mainly to the study of variations of dynamic fracture toughness, K_{IC}^{d}.

In spite of this restriction, indications exist that many controversial phenomena, could be better understood if the relation between strain rate and mechanical properties was taken into account. Especially, for the case of dynamic experiments where the imposed strain rates vary considerably, it is expected that adequate interpretation of experimental data requires consideration of the correct values of the mechanical properties under the strain rates developed. This is by no means avoidable in the case of fast-running cracks, because the propagation of a crack is connected with strong spatial and time variations of the strain field and consequently of the values of the mechanical properties of the material.

In the present study, an attempt was made to determine quantitatively the variations imposed by strain rate on the elastic modulus in the immediate vicinity of running crack tips, and to connect the results with the phenomena of directional instability, such as crack bifurcation.

2. Theoretical analysis

Consider a crack propagating with constant velocity, c, normal to the externally applied load, i.e. under Mode I conditions, in a thin infinite elastic sheet. Because the crack tip changes its position continuously, the stress field developed is time dependent. Hence, a stress- or, equivalently, a strain-rate field is established over the whole sheet. At any point $P(r_0, \theta_0)$ (Fig. 1) the instantaneous value of the dynamic modulus of elasticity, E_d, is defined, by convention in fracture mechanics, through the relation

$$E_d = \left| \frac{\dot{\sigma}(r, \theta)}{\dot{\varepsilon}(r, \theta)} \right| \tag{1}$$

where dots imply differentiation with respect to time and $\dot{\sigma}(r, \theta)$, $\dot{\varepsilon}(r, \theta)$ represent the respective stress- and strain-rate components. The coordinates (r, θ) are functions of time, t, as follows

$$r(t) = [y_0^2 + (x_0 - ct)^2]^{1/2}, \quad \theta(t) = \arctan \frac{y_0}{x_0 - ct} \tag{2a}$$

$$\dot{r}(t) = -\frac{c(x_0 - ct)}{[y_0^2 + (x_0 - ct)^2]^{1/2}},$$

$$\dot{\theta}(t) = \frac{cy_0}{\left[1 + \left(\frac{y_0}{x_0 - ct}\right)^2\right](x_0 - ct)^2} \tag{2b}$$

with (x_0, y_0) indicating the initial cartesian coordinates of point P relative to the moving system (Ox, Oy) (Fig. 1). At this point the normal components of the dynamic stress field, for Mode I loading conditions, are given through Freund and Clifton's formulae [3]

$$\sigma_{\substack{xx \\ yy}}(r, \theta) = \frac{K_I^d}{(2\pi r)^{1/2}} B_I(c) F_{\substack{xx \\ yy}}(c, \theta) \tag{3}$$

0022–2461

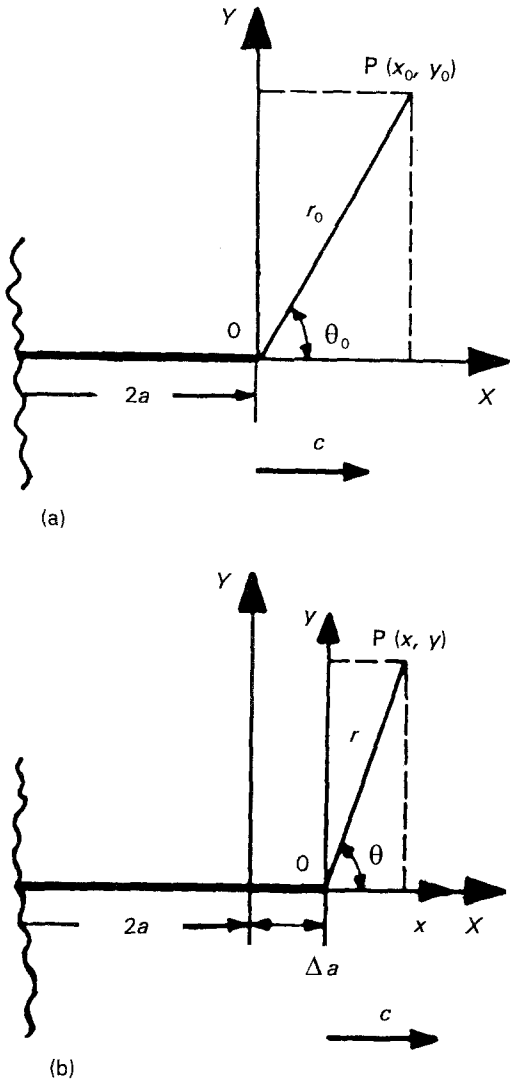

Figure 1 Representation of the geometry of the problem. (a) $t = t_0$, (b) $t = t_0 + \Delta t$.

where

$$B_I(c) = \frac{1 + S_2^2}{4S_1 S_2 - (1 + S_2^2)^2}, \qquad S_{1,2} = 1 - (c/c_{1,2})^2$$

$$F_{xx}(c, \theta) = \left[(1 + 2S_1^2 - S_2^2)f_{11} - \frac{4S_1 S_2}{1 + S_2^2} f_{22}\right],$$

$$F_{yy}(c, \theta) = \left[-(1 + S_2^2)f_{11} - \frac{4S_1 S_2}{1 + S_2^2} f_{22}\right]$$

$$f_{11} = \left\{\left[1 \Big/ \left(1 - \frac{c^2}{c_{1,2}^2 \sin^2\theta}\right)^{1/2}\right] + \left[\cos\theta \Big/ \left(1 - \frac{c^2}{c_{1,2}^2 \sin^2\theta}\right)\right]\right\}^{1/2}$$

In these relations K_I^d is the instantaneous value of Mode I dynamic stress intensity factor and c_1 and c_2 are the dilatational and distortional stress-wave velocities, respectively.

Differentiation of Equation 3 results, after some algebra, in the following expressions for the time derivatives of σ_{xx} and σ_{yy}

$$\dot{\sigma}_{xx} = \frac{K_I^d}{(2\pi r)^{1/2}} \frac{c(x_0 - ct)}{2r^2} \times \left[(1 + 2S_1^2 - S_2^2)f_{11} - \frac{4S_1 S_2}{1 + S_2^2} f_{22}\right] + \frac{K_I^d}{(2\pi r)^{1/2}} \left\{\frac{1 + 2S_1^2 - S_2^2}{2f_{11}} \left[\frac{\gamma\dot{\theta}(t)\sin 2\theta}{2(1 - \gamma\sin^2\theta)^{3/2}} - \frac{\dot{\theta}(t)\sin\theta(1 - \gamma\sin^2\theta) - 2\dot{\theta}(t)\gamma\cos^2\theta\sin\theta}{(1 - \gamma\sin^2\theta)^2}\right] - \frac{4S_1 S_2}{1 + S_2^2} \frac{1}{2f_{22}} \left[\frac{\delta\dot{\theta}(t)\sin 2\theta}{2(1 - \delta\sin^2\theta)^{3/2}} - \frac{\dot{\theta}(t)\sin\theta(1 - \delta\sin^2\theta) - 2\dot{\theta}(t)\delta\cos^2\theta\sin\theta}{(1 - \delta\sin^2\theta)^2}\right]\right\} \tag{4a}$$

$$\dot{\sigma}_{yy} = \frac{K_I^d}{(2\pi r)^{1/2}} \frac{c(x_0 - ct)}{2r^2} \times \left[-(1 + S_2^2)f_{11} + \frac{4S_1 S_2}{1 + S_2^2} f_{22}\right] + \frac{K_I^d}{(2\pi r)^{1/2}} \left\{\frac{1 + S_2^2}{2f_{11}} \left[\frac{\gamma\dot{\theta}(t)\sin 2\theta}{2(1 - \gamma\sin^2\theta)^{3/2}} - \frac{\dot{\theta}(t)\sin\theta(1 - \gamma\sin^2\theta) - 2\dot{\theta}(t)\gamma\cos^2\theta\sin\theta}{(1 - \gamma\sin^2\theta)^2}\right] - \frac{4S_1 S_2}{1 + S_2^2} \frac{1}{2f_{22}} \left[\frac{\delta\dot{\theta}(t)\sin 2\theta}{2(1 - \delta\sin^2\theta)^{3/2}} - \frac{\dot{\theta}(t)\sin\theta(1 - \delta\sin^2\theta) - 2\dot{\theta}(t)\delta\cos^2\theta\sin\theta}{(1 - \delta\sin^2\theta)^2}\right]\right\} \tag{4b}$$

where $\gamma = c^2/c_1^2$ and $\delta = c^2/c_2^2$.

Under plane stress conditions, Equation 1 takes the form

$$\dot{\varepsilon}_{xx} = \frac{1}{E_d}[\dot{\sigma}_{xx}(r, \theta) - \nu\dot{\sigma}_{yy}(r, \theta)] \tag{5}$$

where ν is the Poisson's ratio of the material. In the following text, for simplicity, the coordinates (r, θ) will be omitted.

Equation 5 establishes a relationship between the five quantities $\dot{\sigma}_{xx}$, $\dot{\sigma}_{yy}$, $\dot{\varepsilon}_{xx}$, ν and E_d. The first two of them are analytically known through Equations 4a and b. Also an experimental relationship between $\dot{\varepsilon}_{xx}$ and E_d is given by Theocaris and Andrianopoulos [4] for a wide range of strain-rate values and for two materials, PMMA and PCBA. A computer simulation of this curve for PMMA, by means of spline interpolation, is represented in Fig. 2. From the same series of experiments, it has been proved that the Poisson's ratio of both materials remains essentially constant versus strain rate. Thus, if we assign to ν its mean value, only the respective value of $\dot{\varepsilon}_{xx}$ at every point and time must be known, in order to compute the value of E_d. Because, however, Equation 5 includes two unknown quantities (E_d and $\dot{\varepsilon}_{xx}$), the following iterative procedure of successive approximations is established, with the aid of Equation 5 and Fig. 2.

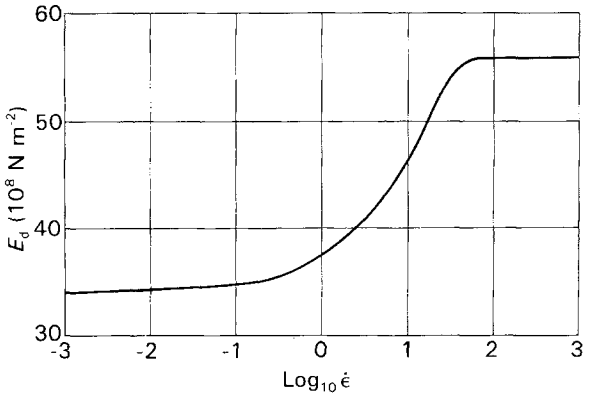

Figure 2 A computer simulation of the experimental $E_d = E_d(\dot{\epsilon}_{xx})$ curve.

(i) The static value, E_{st}, is assigned to E_d.

(ii) Initial values of stress-wave velocities c_1 and c_2 are obtained from the following equations [5]

$$c_1 = \{E_d/[\rho(1 - \nu^2)]\}^{1/2} \quad (6a)$$

$$c_2 = \{E_d/[2\rho(1 + \nu)]\}^{1/2} \quad (6b)$$

where ρ is the mass density of the material.

(iii) Equations 3 and 4 yield the initial values for the dynamic stresses and their time derivatives.

(iv) A first approximation of $\dot{\epsilon}_{xx}$ is obtained through Equation 5.

(v) An improved value of E_d is obtained with the aid of Fig. 2 and an internal loop, including Steps (iv) and (v), is established until convergence of E_d values is obtained.

(vi) The external loop begins again from Step (ii) by computing new improved values of c_1 and c_2 through Equations 6a and b for the corrected value of E_d obtained in Step (v).

3. Application and results

The iterative method described above was applied for PMMA with a static value of elastic modulus $E_{st} = 3.4 \times 10^8$ Pa, initial stress-wave velocities $c_1 \simeq 1800\ \mathrm{m\,s^{-1}}$, $c_2 \simeq 1030\ \mathrm{m\,s^{-1}}$ and the function $E_d = E_d(\dot{\epsilon}_{xx})$ given in Fig. 2. The maximum divergence allowed for c_1 was 10 Pa and for c_1 was $1\ \mathrm{m\,s^{-1}}$. The dynamic stress intensity factor, K_d^d, was calculated by its static value and corrected with the appropriate velocity correction factor, $K(c)$ [6]. Because only the singular terms of Freund and Clifton's formulae have been used for the computation of the stress components, attention was paid to restrict our investigations in the immediate vicinity of the crack tip, i.e. in the region where $a/r < 20$ (a is the length of the crack). It was found that for the case of PMMA, the method converges fast enough.

In Fig. 3a and b the variation of the dynamic elastic modulus and the respective strain rate, with continuous and dotted lines, respectively, is plotted versus time and reduced distance of the point from the crack tip, for a crack velocity equal to $0.35c_2$. The origin of time was taken as the moment at which the crack tip lies exactly below the studied point, P.

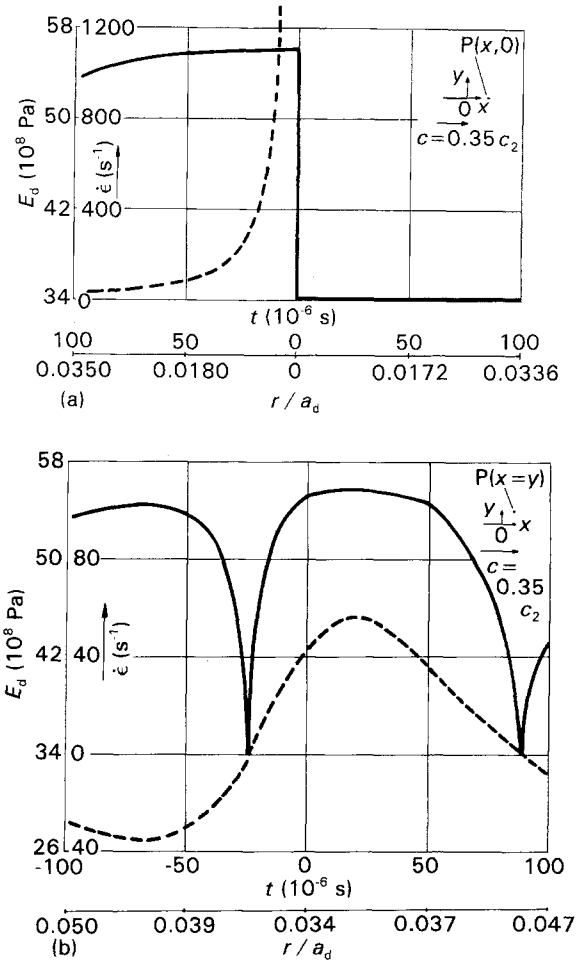

Figure 3 Dynamic modulus of elasticity and (---) strain rate versus time and reduced distance. (a) $(x_0, y_0) = (0.035a, 0)$. (b) $(x_0, y_0) = (0.035a, 0.035a)$.

The fixed point, P, in Fig. 3a has as initial coordinates $(x_0, y_0) = (0.035a, 0)$, i.e. it lies at a distance, x_0, equal to $0.035a$ straight ahead of the initial crack-tip position. In this figure, both E_d and $\dot{\epsilon}_{xx}$ increase rather rapidly as the crack tip approaches the studied point P, and in the limit where the point P coincides with the crack tip, the strain rate tends to infinity and the dynamic modulus attains its ultimate dynamic value $E_d = 55.9 \times 10^8$ Pa. Then, as the tip leaves the point P behind, there is a drop in the value of elastic modulus to its static value, E_{st}, and of strain rate to zero, as expected.

In Fig. 3b, the initial coordinates (x_0, y_0) of point P are $(0.035a, 0.035a)$. As is clear from this figure, the strain-rate curve presents at least two zeroing points in the region of validity of the singular Freund and Clifton's formulae, while at the same points the elastic modulus shows its minimum (static) value. It is worth noting that the first zeroing point does not correspond to the moment when the crack tip lies exactly below point P, but early enough.

So, we observe that in the close vicinity of the crack tip, there exist points under a static elastic modulus together with points under highly dynamic values of the same modulus.

Fig. 4 gives the instantaneous radial distribution of E_d along five characteristic angular directions and for a crack velocity equal to $0.35c_2$. As the distance from

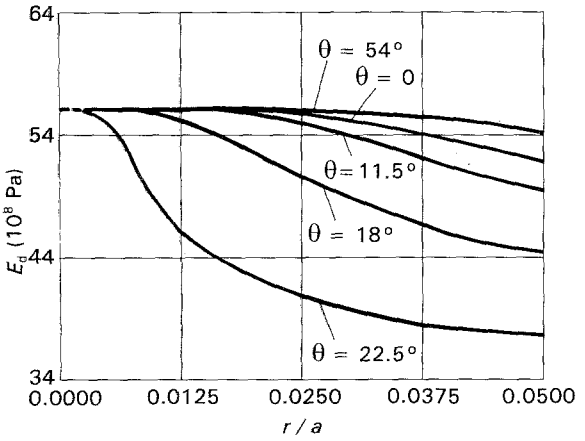

Figure 4 Radial distribution of dynamic modulus of elasticity for some characteristic directions. t = constant, $c = 0.35c_2$.

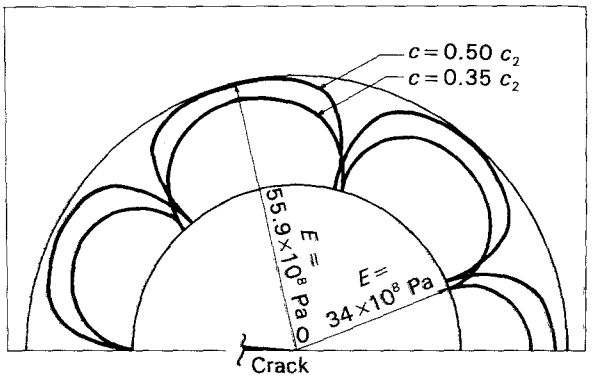

Figure 5 Polar distribution of dynamic modulus of elasticity at a distance r from the crack tip equal to $0.0375a$.

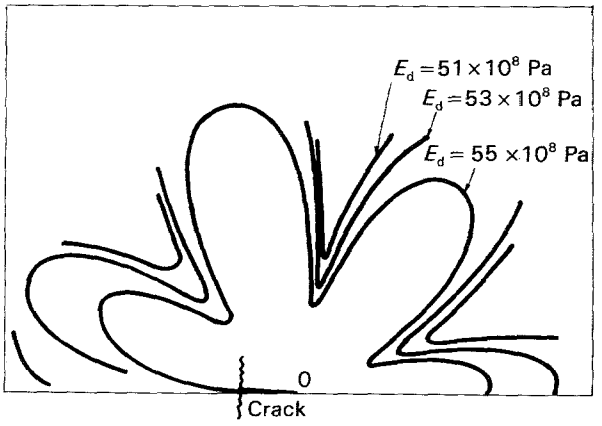

Figure 6 Curves of equal value of dynamic modulus of elasticity, $c = 0.35c_2$.

the crack tip increases. E_d drops monotonically from its maximum value $E_d = 55.9 \times 10^8$ Pa, common for all these directions, to its static value. It should be emphasized that the two outer curves, i.e. for $\theta = 22.5°$ and 54.0°, form a band of E_d values, where for a given distance from the crack tip, the dynamic elastic modulus varies. The same conclusion may be drawn from Fig. 5, where the polar distribution of E_d is plotted for two characteristic crack velocities, i.e. $c = 0.35c_2$ and $0.50c_2$. It should be emphasized that due to symmetry, only the upper half of the curves has been plotted. The polar distribution exhibits seven axes of almost symmetry with period roughly equal to $\pi/7$, the exact value of it depending slightly on the crack velocity. Along these seven axes, where extreme values of E_d appear, the following condition is satisfied

$$\frac{\partial \dot{\varepsilon}_{xx}}{\partial \theta} = 0 \tag{7a}$$

or

$$\frac{\partial^2 \varepsilon_{xx}}{\partial \theta \partial t} = 0 \tag{7b}$$

or

$$\frac{\partial^2 \varepsilon_{ii}}{\partial \theta \partial t} = 0 \tag{7c}$$

These equations can be considered as constituting a strain criterion for crack path deviation, because at points satisfying it, the highest spatial and time strain rates appear, provided also that a minimum value for E_d corresponds to these points. Really the closest to the crack-axis point satisfying Equation 7 and having a minimum value of E_d lies at a direction of about 22.5° to the crack axis (which only slightly depends on velocity), a value close enough to most experimental data for branching angles.

The physical content of the above strain criterion is better understood taking into consideration that for a given load or stress level, the dilatational strain-energy density is higher, the higher are the normal strains, or the lower the elastic modulus becomes. However, according, to the T-criterion of fracture [7], the direction of maximum dilatational strain-energy density coincides with the direction at which cracks propagate.

Identical conclusions to those of Fig. 5 can be obtained from Fig. 6, where curves of equal E_d values are plotted around the crack tip, i.e. the curves $E_d = 55 \times 10^8$, 53×10^8 and 51×10^8 Pa. For symmetry reasons again, only the upper half of the curves is plotted.

A similar conclusion supporting the present thesis concerning crack-path deviations has been proposed by Theocaris and Andrianopoulos [4], who stated that, due to the variation of E_d during crack propagation, the energy absorbed by the crack-propagation process may be lower or higher, when compared to its static value. Thus, in order to maintain the stable energy value, the crack will either accelerate or bifurcate in the first case, or it will be momentarily decelerate and, at the extreme, it may be arrested, or stopped in the latter one.

Finally, it should be emphasized that the only hypothesis involved in the present study is that concerning the linear elastic behaviour of the material, which is adopted in order for the Freund and Clifton stress formulae to be valid. However, especially for the case of PMMA, this hypothesis seems to be very tolerable.

4. Conclusion

As a concluding remark, we notice that an accurate description of the crack-path instability phenomena should take into account, beyond the assumed perfect structure of the material, the local inhomogeneities.

This term encompasses not only pre-existing structural deviations but also those caused by the crack-propagation process itself. The former factor has been studied qualitatively by many investigators (the work by McClintock [8] and Ravi Chandar and Knauss [9] is mentioned) and recently was simulated by a flexible quasi-macroscopic model by Theocaris *et al.* [10], resulting in theoretical predictions in very good agreement with experimental evidence. The second factor studied here, drives to compatible predictions, thus enforcing the central idea of a tight relationship between crack-path instability and local inhomogeneity.

In addition, recent studies [11] concerning the second factor producing local inhomogeneities, i.e. the temperature field created around the propagating tip, indicate that thermal phenomena, caused by crack propagation, work similarly, implying that a unified approach including pre-existing and produced local structural deviations, is required by the nature of the crack-path deviations phenomena in order to obtain a clear picture of the mechanisms governing its genesis and development.

References

1. D. F. MARSHALL, *Proc. Phys. Soc.* **20** (1957) 1033.
2. P. S. THEOCARIS and Ch. GEORGIADIS, *Eng. Fract. Mech.* **20** (1984) 75.
3. L. B. FREUND and R. J. CLIFTON, *J. Elasticity* **4** (1974) 293.
4. P. S. THEOCARIS and N. P. ANDRIANOPOULOS, in "Proceedings of the 7th International Conference on Experimental Stress Analysis," edited by A. Betser (Technicon, Haifa, Israel, 1982) pp. 473–82.
5. H. KOLSKY, "Stress Waves in Solids" (Dover, New York, 1963).
6. L. F. ROSE, *Int. J. Fract.* **12** (1976) 799.
7. P. S. THEOCARIS and N. P. ANDRIANOPOULOS, *Eng. Fract. Mech.* **16** (1982) 425.
8. R. M. McCLINTOCK, *Int. J. Fract.* **4** (1968) 101.
9. K. RAVICHANDAR and W. G. KNAUSS, *ibid.* **22** (1984) 65.
10. P. S. THEOCARIS, N. P. ANDRIANOPOULOS and S. K. KOURKOULIS, *Eng. Fract. Mech.* **34** (1989) 1097.
11. P. S. THEOCARIS, S. K. KOURKOULIS, and N. P. ANDRIANOPOULOS, *Int. J. Solids Structures* **29** (1992) 187.

Received 21 July 1992
and accepted 11 January 1993